To what extent is group theory a reliable alternative method of measuring similarities between crystalline materials?

An Extended Essay in Mathematics

September 2025

IB Student Code:

Word Count: 4000 words

Citation Style: MLA 9th Ed.

Picture of a Crystal Exhibiting a Hexagonal Crystal System

Table of Contents

1 Introduction.....3

1.1 Background.....3

1.2 Significance and Outline.....4

2. Group Theory in Crystallography.....5

2.1 Fundamental Concepts of Group Theory.....5

2.2 Point Groups and the Crystallographic Restriction Theorem.....7

3. Mathematical Derivation of Formulas.....9

3.1 Lattice Mapping.....9

3.2 Atomic Mapping.....11

3.3 Symmetry Based Geometric Cost Function.....13

4. Application of Formulas in Modeling.....15

4.1 Selection of Structure and Sample Crystals.....15

4.2 Calculation of Lattice Deformation Cost.....17

4.3 Calculation of Atomic Deformation Cost.....19

4.4 Cost Function and Identification of Unknown Specimen.....20

5. Comparison with Traditional Laboratory Techniques.....21

5.1 Raman Spectroscopy in Structural Analysis.....21

5.2 Energy Dispersive Spectroscopy (EDS).....22

5.3 Advantages and Limitations of Practical vs. Theoretical Methods.....23

6. Conclusion.....24

6.1 Summary of Findings.....24

6.2 Implications for Crystallographic Research.....25

6.3 Future Directions.....25

7.References……26

1 Introduction

1.1 Background

For a long time, I have had a profound interest in crystallography, the "branch of science devoted to the study of molecular and crystalline structure and properties"(Chapuis, 2024). A summer experience in a research center, where I had the opportunity to analyze mineral specimens, brought my attention towards the mathematical analysis in crystallography. As I conducted research, I learned that many mathematicians studied the geometric properties of crystal structures, not only because the elegance of symmetry, but also to investigate their application in the field of physics, chemistry, and material science. The structure of a crystal not only demonstrates its molecular configurations but also determines its macroscopic properties.

In the field of crystallography, analysis of crystal structures is often required for scientists to compare the similarity across specimens to identify them. Currently, scientists use practical methods such as Raman Spectroscopy, where vibrations are reflected from scattered photons, and Energy Dispersive Spectroscopy (EDS), which analyzes X-rays emitted from specimens. However, such methods often require precisely calibrated, expensive equipment which is strictly forbidden from home laboratories and independent research.

As an enthusiast, I seek for an alternative mathematical method to analyze the properties of unknown crystal structure for the purpose of identification and classification. Group theory, a branch of abstract algebra that studies the relationship between a group of elements, will serve as the main tool. While traditional geometric approaches compare structures based on combinatorial transformations, they often fail to distinguish between volumetric and rotational distortions.

Group theory utilizes tools such as point groups and symmetry operators to focus on more meaningful differences, reducing extensive preprocessing of data, and making it easier to apply the analysis on sophisticated datasets.

1.2 Significance and Outline

This essay seeks to investigate the research question **“To what extent is group theory a reliable alternative method of measuring similarities between crystalline materials?”**. Measuring the similarity between crystal structures in micro level has always been a challenge in crystallography. This research is significant as it provides an accurate, cost-friendly and non-destructive method to this question, demonstrating how abstract algebra can be applied to solve real-world problems.

First, the essay will explain the basic concepts of group theory and how it can be used to analyze crystallography. Next, the essay will investigate how geometric and symmetric adapted group theory formulas can be derived mathematically, and a symmetry-adapted cost function will be used to quantify the similarity index between different crystal structures. Then, the cost function will be used to model and identify crystal structures. Finally, this method will be compared with traditional laboratory techniques such as Raman and EDS, assessing practical reliability and limitations of both methods in real-life scenarios.

2. Group Theory in Crystallography

2.1 Fundamental Concepts of Group Theory

Group theory is a field of abstract algebra that studies groups. A group is a collection of finite or infinite elements with a binary operation that can be applied to them. A group satisfies four fundamental properties, as listed below:

Closure: For every two elements in a group, the result of their multiplication is also an element in the group:

$$X, Y \in G \Longrightarrow X * Y \in G$$

Associativity: The associative law of multiplication is valid in a group:

$$X, Y, Z \in G \Longrightarrow (X * Y) * Z = X * (Y * Z)$$

Identity Element: There exists an identity element E, for that a multiplication of any element within the group with E leaves the element unchanged:

$$\exists E \in G such\ that\ \forall X \in G, E * X = X * E = X$$

Inverse Element: For each element in a group, its reciprocal element is also an element of the group, and the result of their multiplication is the identity element:

$$\forall X \in G, \exists X-1 \in G such\ that\ X * X^{-1} = X^{-1} * X = E$$

Other than these properties, group theory also has certain advantages when dealing with multiple coordination systems. Elements in a group can be classified in conjugate pairs using similarity transformations, which describes a change of basis or a symmetry operation. Geometrically, each conjugate pair refers to structurally equivalent element seen from two different reference points, and one can be transformed to the other by symmetry operations (explained in 2.2) exclusively. The formula,

$$B = X^{-1} AX \quad (2.1.1)$$

expresses matrix B as the transformation of A under the basis change defined by X, with A and B referring to symmetry operations. Note that X^{-1} and X cannot be canceled because the group in non-Abelian and the order of multiplication matters.

For example, let A represent a reflection over the x-axis, where multiplying any point (x, y) with A transforms it into $(x, -y)$:

$$A=\begin{pmatrix}1 & 0\\ 0 & -1\end{pmatrix}$$

If the coordination system is rotated 90° clockwise, we would multiply A by the rotation matrix X and its inverse X^{-1}:

$$X=\begin{pmatrix}0 & 1\\ -1 & 0\end{pmatrix}, X^{-1}=\begin{pmatrix}0 & -1\\ 1 & 0\end{pmatrix}$$

The equivalent rotation in the new system will become:

$$B=X^{-1}AX¿\begin{pmatrix}0 & -1\\ 1 & 0\end{pmatrix}\begin{pmatrix}1 & 0\\ 0 & -1\end{pmatrix}\begin{pmatrix}0 & 1\\ -1 & 0\end{pmatrix}¿\begin{pmatrix}-1 & 0\\ 0 & 1\end{pmatrix}$$

This represents a reflection over the y-axis, where multiplying any point (x, y) with B transforms it into $(-x, y)$. Notice that after a rotation of 90° clockwise, a reflection over the x-axis in the original system is identical to a y-axis reflection in the rotated system. This formula will be particularly useful when analyzing crystallography structures, as it allows equivalence of symmetry operations expressed in different coordinate systems, reducing redundancy and excessive calculation.

2.2 Point Groups and the Crystallographic Restriction Theorem

In this paper, point groups will be applied to analyze the symmetry of molecule models within crystallographic unit cells. A point group is the set of symmetrical operations that results in an identical conformation of a lattice with at least one point fixed in an oriented Euclidean space. The fundamental isometries required to create a point group are listed in Table 1. below.

Table 1. Symmetry Operations in Three-Dimensional Point Groups

Operation	Symbol	Description
Identity	I	The identity operation where no transformation takes place.
Rotation	C_n	The rotation about an axis of symmetry by an angle of 2π/n.
Reflection	σ	A mirror projection across the plane where points are mapped symmetrically across the plane.
Inversion	i	The operation that maps every point r in space to its opposite point through a fixed center.
Improper Rotation	S_n	A rotation followed by a reflection through a plane perpendicular to the axis of rotation.

While space groups extend point groups by including translational symmetry, it is unnecessary to consider translational operations in this paper as crystals are arranged periodically, and such actions do not affect the internal symmetry of crystal structures. Therefore, I will be focusing on point group comparison to identify and analyze unit cell structures.

In total, there are 32 point-groups in three dimensions, also known as crystal classes, that exist in crystallography structures and are consistent with translational periodicity. Determined by the number of rotational axes, the number of point groups for each system reflects the variety of similarity operations that can occur in a unit cell. The table of groups are shown in Table 2:

Table 2. The 32 Point Groups in Three Dimensions

Crystal System	Rotation Axis (n)	Number of Point Groups
Triclinic	1	2
Monoclinic	2	3
Orthorhombic	2	3
Tetragonal	4, 2	7
Trigonal	3	5
Hexagonal	6, 3, 2	7
Cubic	4, 3, 2	5

Note that all existing point groups must satisfy the crystallographic restriction theorem, which limits the types of symmetries possible in periodic crystal structures. The theorem states that the angle between the original and rotated vector in a crystal lattice must be rational. This angle θ can be derived using dot product of the two vectors:

$$\vec{v} \cdot R(\vec{v}) = |\vec{v}|^2 \cos\theta \quad (2.2.1)$$

where $\vec{v}$ is a lattice vector and $R(\vec{v})$ is its rotated version.

Since the left-hand side of (2.1) represents an integer multiple of the lattice spacing, the right-hand side should also be rational, so cos θ must be rational.

$$\cos(\theta) \in Q \quad (2.2.2)$$

For a rotational operation C_n, the angle between vectors can be expressed as $\theta = \frac{2\pi}{n}$. Substituting this into (2.2) yields:

$$\cos\left(\frac{2\pi}{n}\right)\in Q \quad (2.2.3)$$

Solving this equation mathematically shows that that rotational symmetries of a crystal are restricted to C_n where n = 1, 2, 3, 4, 6. This theorem will help limit the possible symmetry operations in my point group models, which reduces computational complexity and improves accuracy of the model.

3. Mathematical Derivation of Formulas

In this section, I attempt to investigate a formula to describe the relationship between the point group forms of atoms in two crystals. Let there be sample structure C_1 and unknown structure C_2. The aim of these cost functions is to proceed a series of transformations and operations which maps the atoms of C_2 exactly onto C_1 while minimizing the degree of deformation, where this degree of deformation allows a quantification of the similarity between the two structures.

3.1 Lattice Mapping

The purpose of lattice mapping is to rotate and deform C_2 until a shared lattice exists between two structures, so their atoms can be expressed in the same coordinates and directly compared. First, the lattice of C_2, represented as L_2, will be mapped onto the lattice of C_1, L_1, using the deformation gradient tensor F:

$$L_1 = FL_2 \quad (3.1.1)$$

The tensor F is a unique product of a rotation matrix Q, and a left stretch tensor with positive determinant V, so by polar decomposition, the original equation can be written as

$$L_1 = VQL_2 \quad (3.1.2)$$

To quantify the deformation required to transform C_2 to C_1, the biot strain tensor B is derived by subtracting the 3x3 identity matrix I from the left stretch tensor. Notice that when there is no deformation, V = I, which implies that B = 0. In general, the tensor is defined as

$$B = V - I \quad (3.1.3)$$

where the identity matrix in 3D plane is written as

$$I = \begin{bmatrix} 1 & 0 & 0 \\ 0 & 1 & 0 \\ 0 & 0 & 1 \end{bmatrix}$$

However, also notice that there are infinitely many valid lattice mappings between two crystals, as different lattice matrices can still represent the same set of points in space. For example, the 2D matrices $\begin{bmatrix} 1 & 0 \\ 0 & 1 \end{bmatrix}$ and $\begin{bmatrix} 1 & 1 \\ 0 & 1 \end{bmatrix}$ both describe the same square lattice, since one can be derived from the other after a unimodular transformation. This implies that when transforming crystal structure to lattice matrix, multiplying the matrix by a

unimodular integer matrix N always yields in the same result. This leads to the more general equation of

$$L_1 N = V^{(N)} Q^{(N)} L_2 \quad (3.1.4)$$

where N strictly follows

$$N \in Z^{3x3},\ det(N) = \pm 1$$

In the natural world, crystals form in different sizes depending on crystal system, bonding type, and formation conditions. To enable comparison between two crystal structures with different unit cell size, the lattice matrices are further generalized to supercells by multiplying it with a supercell transformation matrix T:

$$S_1 = L_1 T_1 \quad (3.1.5)$$

where T_1 strictly follows

$$T_1 \in Z^{3x3},\ \ det(T_1) > 1$$

For example, if C_1 has 2 atoms per unit cell and C_2 has 6 atoms per cell, L_1 should be expanded into a larger supercell of three times its original size, which can be derived from multiplying a determinant-three matrix.

The final lattice mapping formula between two crystals is expressed as

$$S_1 N = L_1 T_1 N ¿ V^{(N)} Q^{(N)} L_2 ¿ F^{(N)} L_2 \quad (3.1.6)$$

This counts all possible transformation matrices that link structures C_2 and C_1. However, many of them are equivalent due to iterative counting and symmetry. As in eq.(3.1.5), cells are transformed into supercells, yet one

supercell can be written in many ways. Every unique supercell can be isolated by using the Hermite Normal Form (HNF) for future references. We can also reduce the number of matrices N in eq.(3.1.6) to those that are symmetrically distinct. Let the point group symmetry operations $G^{(1)} \wedge G^{(2)}$ be the set of transformations that leave the crystal lattice unchanged. Though G is in cartesian form, they can also be rewritten in fractional form J using similarity transformation as in eq.(2.1.1):

$$J = L^{-1} G L \quad (3.1.7)$$

We can then rewrite eq.(3.1.6) into

$$G^{(1)} S_1 \left(J^{(1)}\right)^{-1} N = F^{(N)} G^{(2)} L_2 \left(J^{(2)}\right)^{-1} \quad (3.1.8)$$

rearranging eq.(3.1.8) yields

$$S_1 \left(J^{(1)}\right)^{-1} N J^{(2)} = (G¿¿(1))^{-1} F^{(N)} G^{(2)} L_2 ¿ \quad (3.1.9)$$

Writing it in the standard form yields

$$S_1 M = F^{(M)} L_2 \quad (3.1.10)$$

where

¿

3.2 Atomic Mapping

Even if two crystals have matching lattices, their atomic displacements within the unit cell can be arranged differently. Each atom in the standard crystal, C_2, must be mapped to a corresponding atom in the sample crystal, C_1. From eq.(3.1.6), all atoms from C_2 have already experienced a

translation, a rotation, and a stretch. In C_2, the point position for the j^{th} atom can be shown as

$$VQ\left(\overrightarrow{r_j^{(2)}}-\vec{t}\right) \quad (3.2.1)$$

This position derived is then compared with the point position of the i^{th} atom in the parent structure, C_1, with symbol $r_i^{(1)}$. The raw displacement vector

$$r_i^{(1)}-VQ\left(r_j^{(2)}-t\right) \quad (3.2.2)$$

shows the distance between atoms in the two crystal structures. However, since crystals exist as periodic lattice structures, their atoms repeat infinitely in space in specific patterns. This means that for an atom in position *(x, y, z)*, it is equivalent to being at

$$\left(x+n_1 a, y+n_2 b, z+n_3 c\right) \quad (3.2.3)$$

$$n_1, n_2, n_3 \in Z$$

The minimal distance between all possible positions is calculated using the rounding operation, $\lfloor \cdot \rceil_{S_1}$, that takes the positional value in a specific range after converting such distance into fractional coordinates. Therefore, the minimum periodic distance between the i^{th} atom in C_1 and the j^{th} atom in C_2, denoted as, is calculated as

$$d_{i,j}^{(1)}(t)=\lfloor r_i^{(1)}-VQ\left(r_j^{(2)}-t\right)\rceil_{S_1} \quad (3.2.4)$$

where

$$\begin{cases} ¿\, d_{i,j}^{(1)}(t) = minimum\, periodic\, distance\, vector \\ ¿\, r_i^{(1)} = position\, of\, atom\, i \in C_1 \\ ¿\, r_j^{(1)} = position\, of\, atom\, j \in C_2 \\ ¿\, V = strain\, operator \\ ¿\, Q = rotation\, operator \\ ¿\, t = translation\, operator \end{cases}$$

Next, we need to solve the order in which the atoms in C_2 are paired to atoms in C_1. To find the overall minimum distance, permutation is used to create a bijection between a total number of n_A atoms with one-to-one correspondence

$$\hat{p}: \{1, \ldots, i, \ldots, n_A\} \to \{1, \ldots, j, \ldots, n_A\} \quad (3.2.5)$$

where each atom i in C_1 corresponds to atom $\hat{p}[i]$ in C_2.

3.3 Symmetry Based Geometric Cost Function

The next step is to use geometry and symmetry to define cost functions to measure the complexity of such mapping.

First, the shape change during such operations should be isolated from volume change. We can renormalize the left stretch tensor V to make it independent of volume. The determinant of V gives the relative volume change during the mapping process:

$$detV = \frac{V_{C_2}}{V_{C_1}} \quad (3.3.1)$$

The three-dimensional factor is rescaled into one dimension:

$$\widetilde{V}=\frac{V}{det(V)^{1/3}} \quad (3.3.2)$$

This also updates the biot strain tensor from (3.1.3) as

$$\widetilde{B}=\widetilde{V}-I \quad (3.3.3)$$

Using this strain tensor, we can derive a deformation cost function of a scalar measure of how much the lattice must deform. The trace function, $tr(\widetilde{B}^2)$, represents the sum of the diagonal entries of $\widetilde{B}^2$, which is the standard measurement of the magnitude of a symmetric tensor. The value is then normalized by multiplying a factor of $\frac{1}{3}$ which averages the result over 3 principal directions in 3D plane. Therefore, for each mapping M, the cost is measured as

$$c_L(M)=\frac{1}{3}tr(\widetilde{B}^2) \quad (3.3.4)$$

where

¿ $c_L(M)=lattice\,deformation\,cost$

¿ $tr(\widetilde{B}^2)=trace\,function\,of\,the\,biot\,strain\,tensor$ ¿

Next, we find a length scale to quantify atomic and lattice distortions using the Wigner-Seitz radius, which is “the radius of a sphere whose volume is equal to the mean volume per atom” (Girifalco 2003, 125).

$$\rho=\left(\frac{3}{4\pi}\Omega_2\right)^{1/3} \quad (3.3.5)$$

The total cost measures the average squared displacement between matched atoms, using the squared Euclidean norm and normalized by the Wigner–Seitz radius ρ_1:

$$c_A(M)=\frac{1}{\rho_1^2 n_A}\sum_i |d^{(1)}_{i,\hat{p}[i]}(t)|^2 \quad (3.3.6)$$

where

$$\begin{cases} ¿\, c_A(M)=atomic\,deformation\,cost \\ ¿\, \rho_1=the\,Wigner-Seitz\,radius\,of\,the\,standard\,crystal \end{cases} ()¿¿\, n_A=number\,of\,atoms\in the\,unit\,cell$$

Finally, the two components of structural difference, lattice cost and atomic cost, can be combined using a user-defined weight parameter.

$$c(M, w_L)=w_L\cdot c_L(M)+(1-w_L)\cdot c_A(M) \quad (3.3.7)$$

The weight parameter w_L can be adjusted to penalize either lattice or atomic deformation cost over the other, allowing the cost function to adapt to the most important aspect of deformation.

4. Application of Formulas in Modeling

Next, we demonstrate how crystal structures can be identified by comparing them to sample structures using cost function. The cost indicates

the similarity between them: the lower cost required for the structure lattice to be transformed into the sample lattice, the more alike they are.

4.1 Selection of Structure and Sample Crystals

To begin the analysis, we first selected an unknown crystal specimen, shown in Fig.1 below.

Fig.1 Picture of unknown crystal specimen

Due to time and equipment constrains, the crystal's atomic coordinates are obtained from the Inorganic Crystal Structure Database (ICSD). Based on its metallic luster and general crystallographic form, we initially hypothesized that the unknown specimen might also correspond structurally to hematite, another common iron-based mineral. The structural data for atomic coordinates of hematite was also retrieved from the ICSD to allow comparison with the hypothesized structure.

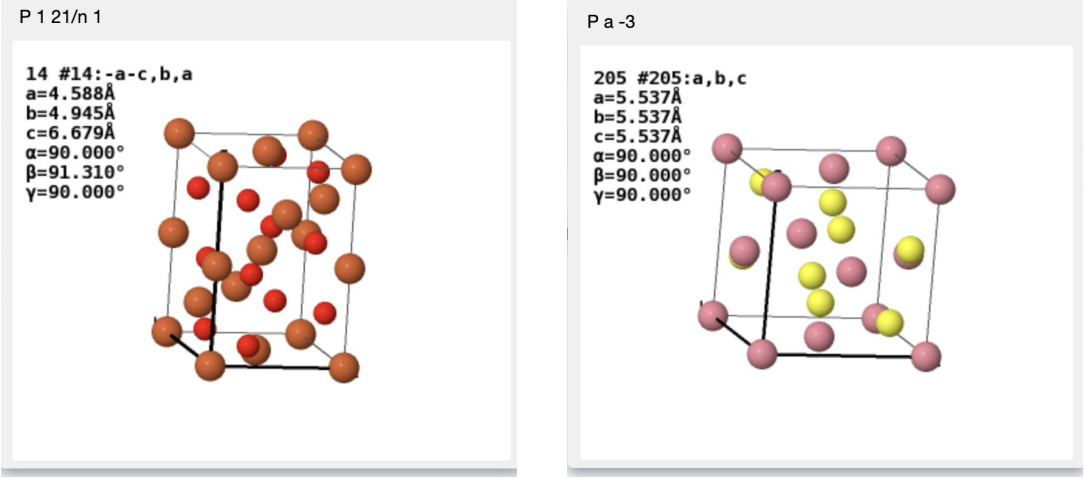

Fig.2 Atomic coordinates of unknown specimen and hematite from ICSD

From the database, the lattice parameters of C_1 and C_2 are listed as below:

$$C_1\begin{cases} ¿\, a_1 = 4.588\,Å \\ ¿\, b_1 = 4.945\,Å \\ ¿\, c_1 = 6.679\,Å \\ ¿\, \alpha = 90\,° \\ ¿\, \beta = 91.31\,° \\ ¿\, \gamma = 90\,° \end{cases} \qquad C_2\begin{cases} ¿\, a_2 = 5.537\,Å \\ ¿\, b_2 = 5.537\,Å \\ ¿\, c_2 = 5.537\,Å \\ ¿\, \alpha = 90\,° \\ ¿\, \beta = 90\,° \\ ¿\, \gamma = 90\,° \end{cases}$$

Using the standard monoclinic Cartesian convention:

$$a=(a,0,0)\, b=(0,b,0)\, c=(c\cos\beta, 0, c\sin\beta)$$

The corresponding transformation lattice matrix can be represented as follow:

$$L_1=\begin{pmatrix} a_1 & 0 & c_1 cos\beta \\ 0 & b_1 & 0 \\ 0 & 0 & c_1 sin\beta \end{pmatrix}=\begin{pmatrix} 4.588 & 0 & -0.11656 \\ 0 & 4.945 & 0 \\ 0 & 0 & 6.67798 \end{pmatrix} Å \qquad (4.1.1)$$

$$L_2=\begin{pmatrix} a_2 & 0 & c_2 cos\beta \\ 0 & b_2 & 0 \\ 0 & 0 & c_2 sin\beta \end{pmatrix}=\begin{pmatrix} 5.537 & 0 & 0 \\ 0 & 5.537 & 0 \\ 0 & 0 & 5.537 \end{pmatrix}\mathring{A} \quad (4.1.2)$$

L_1 also experiences a basis change $(-a-c, b, a)$, which can be written as transformation matrix T:

$$T=\begin{pmatrix} -1 & 0 & 1 \\ 0 & 1 & 0 \\ -1 & 0 & 0 \end{pmatrix} \quad (4.1.3)$$

We can now derive the supercell S_1 from eq.(4.1.1) and (4.1.3):

$$S_1=L_1\,T_1 ¿ \begin{pmatrix} 4.588 & 0 & -0.11656 \\ 0 & 4.945 & 0 \\ 0 & 0 & 6.67798 \end{pmatrix}\begin{pmatrix} -1 & 0 & 1 \\ 0 & 1 & 0 \\ -1 & 0 & 0 \end{pmatrix} ¿ \begin{pmatrix} -4.588 & 0 & -0.11656 \\ 0 & 4.945 & 0 \\ -6.67798 & 0 & 0 \end{pmatrix} \quad (4.1.4)$$

Their structures can be abstracted as the cubic and tetragonal structure in image below. The cost function maps the cubic lattice onto the tetragonal lattice.

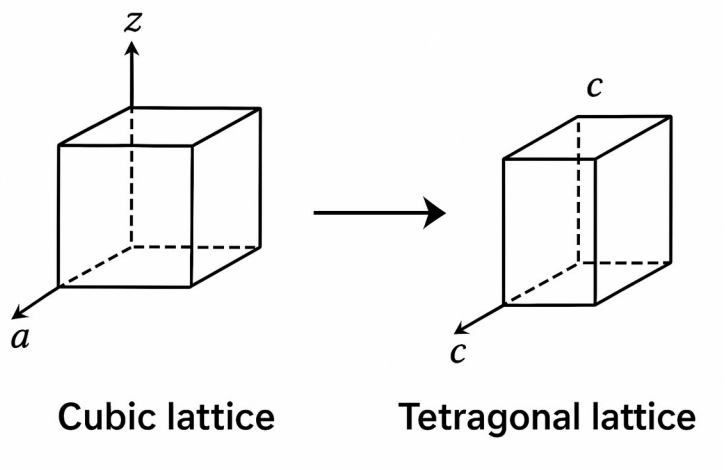

Fig.3 Abstract structure of crystal lattices

4.2 Calculation of Lattice Deformation Cost

Next, the deformation gradient tensor F can be calculated.

$$L_1 = F L_2 \quad (4.2.1)$$

Thus,

$$F = L_1 L_2^{-1} ¿ \begin{pmatrix} \frac{4.588}{5.537} & 0 & 0 \\ 0 & \frac{4.945}{5.537} & 0 \\ 0 & 0 & \frac{6.679}{5.537} \end{pmatrix} ¿ \begin{pmatrix} 0.829 & 0 & 0 \\ 0 & 0.893 & 0 \\ 0 & 0 & 1.207 \end{pmatrix} \quad (4.2.2)$$

In this case, the matrix is diagonal and positive, therefore there is no rotation component, and we can set the rotation vector Q as the identity matrix I. The left stretch tensor V is equal to F.

Next, I compute the determinant of V:

$$det(V) = det(F) ¿ 0.829 \cdot 0.893 \cdot 1.207 \approx 0.894 \quad (4.2.3)$$

Normalizing V using eq.(4.2.3) isolates volume change and gives:

$$\tilde{V} = \frac{V}{det(V)^{1/3}} ¿ \frac{V}{0.894^{1/3}} ¿ \frac{V}{0.962} ¿ \begin{pmatrix} \frac{0.829}{0.962} & 0 & 0 \\ 0 & \frac{0.893}{0.962} & 0 \\ 0 & 0 & \frac{1.207}{0.962} \end{pmatrix} ¿ \begin{pmatrix} 0.862 & 0 & 0 \\ 0 & 0.928 & 0 \\ 0 & 0 & 1.255 \end{pmatrix} \quad (4.2.4)$$

The normalized value can then be used to derive the renormalized biot strain using eq.(3.1.3):

$$\widetilde{B}=\widetilde{V}-1 \quad (4.2.5)$$
¿
$$\begin{pmatrix} 0.862-1 & 0 & 0 \\ 0 & 0.928-1 & 0 \\ 0 & 0 & 1.255-1 \end{pmatrix}$$
¿
$$\begin{pmatrix} -0.138 & 0 & 0 \\ 0 & -0.072 & 0 \\ 0 & 0 & 0.255 \end{pmatrix}$$

Lattice deformation cost can be derived using eq.(3.3.4):

$$c_L(M)=\frac{1}{3}tr\left(\widetilde{B}^2\right) \quad (4.2.6)$$
¿ $\frac{1}{3}((-0.138)^2+(-0.072)^2+(0.255)^2)\approx\frac{1}{3}(0.089)\approx 0.0297$

This small but nonzero lattice cost indicates that the cubic and tetragonal unit cells are close in symmetry but differ by an anisotropic stretch along the z-axis.

4.3 Calculation of Atomic Deformation Cost

To calculate the Wigner–Seitz radius of C_2, we first need to find the number of atoms in each unit cell. The volume of one unit cell is:

$$V_2=a_2^3=5.537^3=169.5\ \text{Å}^3 \quad (4.3.1)$$

The Wigner–Seitz radius is then

$$\rho=\left(\frac{3}{4\pi}\Omega_2\right)^{1/3} \quad (4.3.2)$$
¿ $\left(\frac{3\cdot 169.5}{4\pi}\right)^{1/3}\approx(18.11)^{1/3}\approx 2.62\ \text{Å}$

Atomic deformation cost can be derived using eq.(3.3.6):

$$c_A(M)=\frac{1}{\rho_1^2 n_A}\sum_i |d^{(1)}_{i,\hat{p}[i]}(t)|^2 \quad (4.3.3)$$
¿ $\frac{0.0091}{(2.62)^2\cdot 2}\approx 6.63\times 10^{-4}$

4.4 Cost Function and Identification of Unknown Specimen

Using the cost function

$$c(M, w_L) = w_L \cdot c_L(M) + (1 - w_L) \cdot c_A(M)$$

We can set w_L to 0.5 and find that the similarity index between our two crystal structures is approximately 0.0512. Since the value is heavily dominated by the lattice deformation cost, it suggests that the lattice parameters of C_1 and C_2 differ while the atomic parameters are very similar. In fact, the specimen C_2 I chosen was pyrite. Pyrite and hematite are similar in that both are iron-based minerals with nearly identical arrangements of molecules, which makes their atomic coordinates somewhat analogous. However, they do differ in crystal structure and lattice parameters, as pyrite is cubic with right-angled edges, and hematite has a slightly tetragonal unit cell. Therefore, this result is rather reliable, as it implies that the specimen is not hematite**,** yet it belongs to a similar mineral family with comparable atomic structure**.**

5. Comparison with Traditional Laboratory Techniques

In the previous section, theoretical models of iron isotopes are identified through cost functions. In this section, the results will be compared with the practical results of analyzing a stromatolite sample in atomic level using Raman Spectroscopy and Energy Dispersive Spectroscopy.

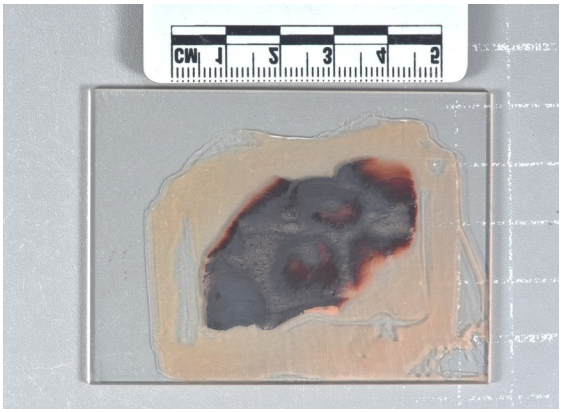

Fig.4 Image of Stromatolite Sample

5.1 Raman Spectroscopy in Structural Analysis

This method illuminates the substance with lasers and analyzes the reflected light after interacting with chemical bonds.

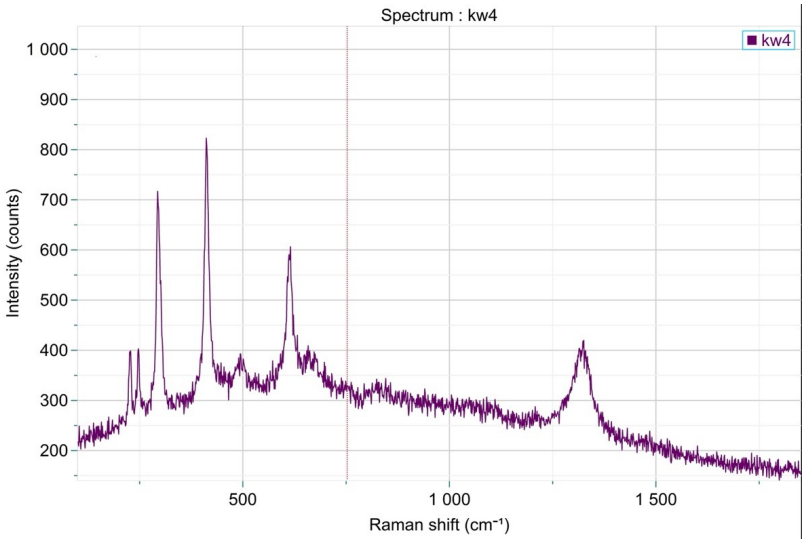

Fig.5 Raman Spectrum of Stromatolite Sample

Reading from Fig.5, the resulting spectrum revealed five significant peaks at approximately 200, 300, 400, 600**,** and 1350 cm^{-1}.

RAMAN Band Correlation Table

Approximate Wavenumber Range (cm−1)	Group	Intensity
100–210	Lattice vibrations	Strong
150–430	Xmetal-O	Strong
250–400	C-C aliphatic chain	Strong
295–340	Se-Se	Strong
425–550	S-S	Strong
460–550	Si-O-Si	Strong
490–660	C-I	Strong
505–700	C-Br	Strong
550–790	C-Cl	Strong
580–680	C=S	Strong
630–1250	C-C aliphatic chains	Moderate
670–780	C-S	Strong
720–800	C-F	Strong
800–950	C-O-C	Weak
910–960	Carboxylic acid dimer	Weak
990–1100	Aromatic rings	Strong
1010–1095	Si-O-C	Weak
1010–1095	Si-O-Si	Weak
1020–1225	C=S	Strong
1025–1060	Sulfonic acid	Very weak
1050–1210	Sulfonamide	Moderate
1050–1210	Sulfonamide	Moderate
1050–1210	Sulfone	Moderate
1120–1190	Si-O-C	Weak
1145–1240	Sulfonic acid	Very weak
1315–1435	Carboxylate salt	Moderate
1320–1350	Nitro	Very strong
1355–1385	C-CH3	Weak
1365–1450	Aromatic azo	Very strong
1405–1455	CH2	Weak
1405–1455	CH3	Weak
1450–1505	Aromatic ring	Moderate
1535–1600	Nitro	Moderate
1540–1590	Aliphatic azo	Moderate
1550–1610	Aromatic/hetero ring	Strong
1550–1700	Amide	Strong
1600–1710	Ketone	Moderate
1610–1740	Carboxylic acid	Moderate
1625–1680	C=C	Very strong
1630–1665	C=N	Very strong
1690–1720	Urethane	Moderate
1710–1725	Aldehyde	Moderate
1710–1745	Ester	Moderate
1730–1750	Aliphatic ester	Moderate

Fig.6 Raman Band Correlation Table

Referring to the band correlation table, the lower wave peaks between 200 to 600 cm^{-1} are consistent with lattice vibrational modes of silicate and hematite minerals, while the peak at 1350 cm^{-1} corresponds to the D-band of disordered carbon, indicating that the sample contains organic carbon. This suggests that the sample is a stromatolite, as it contains a significant amount of mineral components such as silicates, iron oxide, and preserved organic carbon from fossilized micro-organisms.

5.2 Energy Dispersive Spectroscopy (EDS)

The EDS function integrated analyzes and quantifies the element compositions of sample, which is slightly different to the raman result.

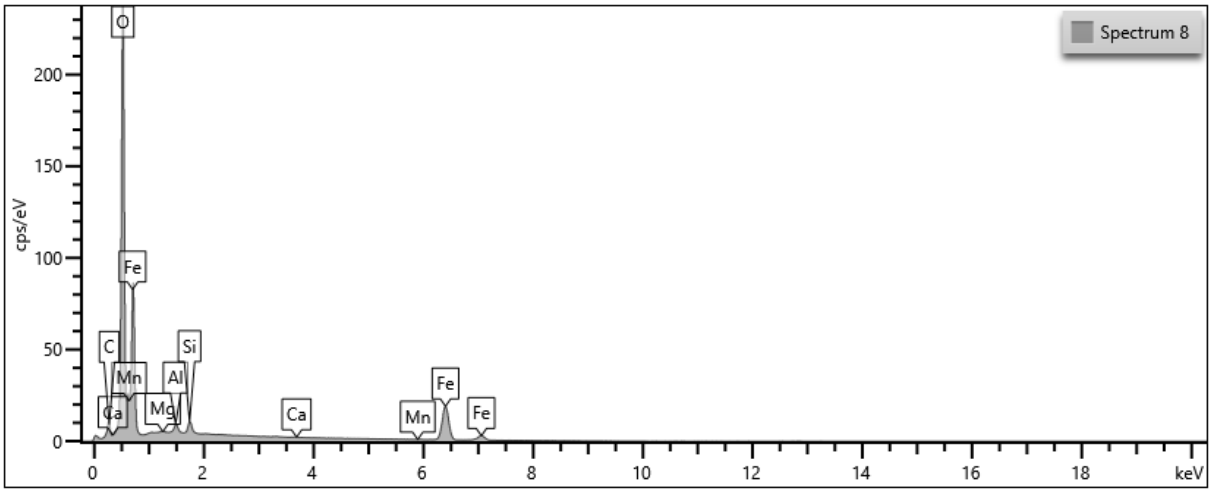

Fig.7 EDS Spectrum of Stromatolite Sample

The spectrum also shows dominant signals for oxygen (O), iron (Fe), carbon (C) and silicon (Si), which form the typical matrix of many hematite stromatolites.

5.3 Advantages and Limitations of Practical vs. Theoretical Methods

Experimental techniques, including Raman spectroscopy and Energy-Dispersive X-ray Spectroscopy, provided direct physical evidence of the sample's chemical and mineralogical composition. These results support the hypothesis that the sample contains carbonate features consistent with stromatolite structures. A key advantage of these methods is their ability to detect real-world complexity, including trace element variation, and mixed-phase mineralogy. However, both methods are qualitative, and interpretation depends heavily on expert comparison with known standards.

In contrast, the theoretical modeling suggested in this essay used to compare crystal structures via symmetry operations and lattice transformations offers a quantitative and reproducible method to assess structural similarity. It allows for the abstraction of crystallographic data into a measurable cost metric, enabling systematic comparison between the sample and known systems. A major strength of this method is its objectivity and generalizability, as it can be applied across a wide dataset and is not limited by experimental noise.

Nonetheless, theoretical models are inherently limited by their assumptions and idealizations. In this case, the model assumes a degree of crystallinity, periodicity, and ideal lattice symmetry, which may not fully capture the heterogeneous features present in natural minerals. Additionally, the model depends on the availability and accuracy of crystallographic input data and may overlook biologically relevant features that do not manifest at the atomic-lattice level.

6. Conclusion

6.1 Summary of Findings

This investigation aimed to evaluate the reliability of group theory as an alternative mathematical method for comparing crystalline materials. Through the derivation and application of a two-part symmetry-adapted cost function, we demonstrated how group transformations, including lattice

mapping, polar decomposition, and atomic permutation, can be used to quantitatively model structural similarities between crystals, transforming structural comparison into a computational optimization problem. The results revealed that many structural differences traditionally attributed to chemical identity or formation environment could be quantitatively expressed as symmetry-breaking transformations, allowing for more general and scalable analysis.

In practical application, the theoretical model was supported by experimental analysis of mineral samples using Raman Spectroscopy and Energy-Dispersive X-ray Spectroscopy. Raman results indicated peaks consistent with hematite and carbon, while EDS confirmed the presence of elemental Fe, Si, O, and C, together supporting the hypothesis that the sample was a stromatolite. These findings collectively validated the group-theoretical framework by correlating its structural predictions with laboratory observations.

6.2 Implications for Crystallographic Research

The integration of group theory into crystallographic analysis offers a promising, mathematically rigorous alternative to traditional physical methods. Unlike experimental approaches that rely on empirical spectra and expert interpretation, modeling enables algorithmic evaluation of structural similarity, regardless of crystal size or orientation. Its abstraction

of crystallographic structures into symmetry-based data reduces dependence on expensive laboratory equipment and makes structural comparison more accessible to independent researchers.

Moreover, the structural distance metric derived in this essay provides a universal, scalar measure of similarity, potentially useful for database searches, automated mineral classification, and modeling of polymorphic transitions. As such, group theory not only complements existing laboratory techniques but can enhance their accuracy and scalability in digital crystallography.

6.3 Future Directions

While the mathematical model in this essay demonstrates strong potential, further development is needed to improve its applicability and resolution. Completing the automation and programming implementation of the cost function algorithm will allow broader comparisons across large crystal structure databases. Future studies could integrate machine learning algorithms to cluster crystals or incorporate space group operations to extend beyond unit cell analysis.

7.References

Thomas, John C., Anirudh Raju Natarajan, and Anton Van der Ven.

“Comparing Crystal Structures with Symmetry and Geometry.” *npj*

Computational Materials, vol. 7, no. 164, 2021, https://doi.org/10.1038/s41524-021-00627-0

Chen, Xiaobing, et al. “Enumeration and Representation Theory of Spin Space Groups.” *Physical Review X*, vol. 14, no. 3, 2024, p. 031038, https://doi.org/10.1103/PhysRevX.14.031038

Watanabe, Haruki, Hoi Chun Po, and Ashvin Vishwanath. “Structure and Topology of Band Structures in the 1651 Magnetic Space Groups.” *Science Advances*, vol. 4, no. 8, 2018, eaat8685, https://doi.org/10.1126/sciadv.aat8685

Song, Zhi, et al. “Structure and Topology of Band Structures in the 1651 Magnetic Space Groups.” *Science Advances*, vol. 4, no. 8, 2018, eaat8685, https://doi.org/10.1126/sciadv.aat8685

Macauley, Matthew. *Math 4120: Modern Algebra.* Clemson University, https://www.math.clemson.edu/~macaule/classes/m20_math4120/. Accessed 10 Sept. 2025

Powell, Richard C. *Symmetry, Group Theory, and the Physical Properties of Crystals.*

Balamuralitharan, S., et al. "Analyzing Symmetry in Group Theory: Applications in Crystallography." *Communications on Applied Nonlinear Analysis*, vol. 31, no. 2, 2024, p. 440

Souvignier, Bernd. *Group Theory Applied to Crystallography.* Institute for Mathematics, Astrophysics and Particle Physics, Radboud University Nijmegen, 29 Apr. 2008.